Estimation of myocardial blood flow and myocardial flow reserve by ^{99m}Tc-sestamibi imaging: comparison with the results of [^{15}O]H_2O PET

Yoshinori Ito[1], Chietsugu Katoh[2], Kazuyuki Noriyasu[1], Yuji Kuge[2], Hideto Furuyama[3], Koichi Morita[3], Tetsuro Kohya[1], Akira Kitabatake[1], Nagara Tamaki[3]

[1] Department of Cardiology, Hokkaido University Graduate School of Medicine, Sapporo, Japan
[2] Department of Tracer Kinetics, Hokkaido University Graduate School of Medicine, Sapporo, Japan
[3] Department of Nuclear Medicine, Hokkaido University Graduate School of Medicine, N-15, W-7, Kita-ku, Sapporo, 060-8638 Japan

Received: 1 July 2002 / Accepted: 19 September 2002 / Published online: 14 November 2002

Abstract. We developed a noninvasive method to quantitatively estimate the myocardial blood flow (MBF) index and flow reserve (MFR) using dynamic and static data obtained with technetium-99m sestamibi, and compared the results with MBF and MFR measured by oxygen-15-labeled water ([^{15}O]H_2O) PET. Twenty patients with coronary artery disease (CAD) and nine normal subjects underwent both ^{99m}Tc-sestamibi and PET studies within 2 weeks. From the anterior view, dynamic data were acquired for 2 min immediately after the injection of ^{99m}Tc-sestamibi, and planar static images were also obtained after 5 min at rest and during ATP stress (0.16 mg kg^{-1} min^{-1} for 5 min) on another day. The area under the time-activity curve on the aortic arch (Aorta ACU), myocardial weight with the SPET image (M), and the myocardial count on the planar image for 1 min (C_m) were obtained. The MBF index (MBFI) was calculated as follows: MBFI=C_m/Aorta ACU×100/M. MFR was measured by dividing the MBFI at ATP stress by MBFI at rest. The MBFI measured by ^{99m}Tc-sestamibi was significantly correlated with MBF obtained using [^{15}O]H_2O PET (MBFI=13.174+11.732×MBF, r=0.821, P<0.001). Furthermore, MFR measured by ^{99m}Tc-sestamibi was well correlated with that obtained using [^{15}O]H_2O PET, with some underestimation (r=0.845, P<0.001). MFR using ^{99m}Tc-sestamibi in patients with CAD was significantly lower than that in normal subjects (CAD: 1.484±0.256 vs normal: 2.127±0.308, P<0.001). These data suggest that the MBFI and MFR can be measured with ^{99m}Tc-sestamibi. This may be useful for the quantitative assessment of CAD, especially in those patients with diffuse coronary disease.

Nagara Tamaki (✉)
Department of Nuclear Medicine,
Hokkaido University Graduate School of Medicine,
N-15, W-7, Kita-ku, Sapporo, 060-8638 Japan
e-mail: natamaki@med.hokudai.ac.jp
Tel.: +81-11-7065150, Fax: +81-11-7067155

Keywords: Radionuclide imaging – Emission tomography – Myocardial blood flow – ^{99m}Tc-sestamibi – Coronary artery disease

Eur J Nucl Med (2003) 30:281–287
DOI 10.1007/s00259-002-1031-y

Introduction

Myocardial perfusion imaging has been widely used for the diagnosis and evaluation of coronary artery disease (CAD) [1, 2, 3, 4, 5]. However, since perfusion imaging documents relative myocardial perfusion, it has limited utility, particularly in patients with multivessel disease or diffuse CAD. Quantitative assessment of myocardial flow reserve (MFR) is valuable for early detection of diffuse coronary disease, estimation of its severity, and assessment of treatment effects. Positron emission tomography (PET) plays a major role in estimating MFR. On the other hand, PET has not been used clinically owing to the limited availability of PET systems and difficulties in the production of PET tracers. If MFR could be estimated with single-photon emission tomography (SPET) and commonly used technetium-99m perfusion tracers, MFR measurement would become widely available for quantitative assessment of coronary function. Recently quantitative assessment of MFR has been attempted with the use of dynamic acquisition following administration of a ^{99m}Tc perfusion agent [6, 7].

We have developed a noninvasive method to quantitatively estimate myocardial blood flow (MBF) and MFR with ^{99m}Tc-sestamibi by taking into account the arterial input function. The goal of this study was to investigate the validity of measurement of MBF and MFR using ^{99m}Tc-sestamibi by comparing the results with those obtained using oxygen-15 labeled water ([^{15}O]H_2O) PET.

Table 1. Data from controls and patients

	Age (yr)	Sex	CAG (%)			RV	MI	SPET	Tc-MBFI (rest)	Tc-cMB FI(rest)	Tc-MB FI (ATP)	Tc-MFR	Tc-cMFR	PET-MB F (rest)	PET-cM BF(rest)	PET-MB F(ATP)	PET-MFR	PET-cMFR
			LAD	LCx	RCA													
Controls																		
1	35	M						–	30.9	26.6	66.8	2.160	2.516	0.738	0.839	3.402	4.610	4.056
2	35	M						–	29.4	28.5	62.6	2.131	2.199	1.025	1.064	3.116	3.040	2.927
3	34	M						–	21.3	18.1	47.0	2.201	2.593	0.843	0.675	3.164	3.753	4.684
4	33	M						–	36.5	27.7	76.5	2.093	2.763	1.108	0.888	3.887	3.508	4.379
5	30	M						–	29.6	30.1	55.3	1.872	1.838	1.224	1.360	3.962	3.237	2.913
6	63	F	–	–	–			+	33.9	26.4	55.8	1.645	2.115	1.185	1.079	4.011	3.385	3.718
7	46	M						–	28.0	27.1	74.4	2.657	2.739	1.084	1.038	5.178	4.777	4.990
8	27	M						–	22.8	18.9	56.7	2.480	2.994	0.749	0.937	3.320	4.433	3.543
9	42	M						–	16.9	15.2	32.3	1.908	2.125	0.674	0.729	2.076	3.080	2.847
Patients																		
1	70	M	75			CABG		+	19.7	19.1	25.0	1.272	1.313	0.886	0.880	1.577	1.780	1.792
2	75	M		90		PTCA	+	–	17.3	18.0	31.9	1.841	1.775	0.834	0.978	2.163	2.594	2.211
3	44	M		75	75			–	29.1	19.1	37.0	1.271	1.939	0.964	0.702	2.031	2.107	2.893
4	76	M	75					+	18.1	17.5	30.5	1.684	1.738	0.772	0.813	1.778	2.303	2.186
5	66	M	100	90	90			+	21.6	15.6	27.1	1.253	1.739	1.094	0.691	1.081	0.988	1.565
6	75	M	90					+	16.8	15.2	23.3	1.390	1.532	0.951	0.974	3.039	3.196	3.119
7	69	M	90	75	90	PTCA	+	–	22.0	18.8	28.2	1.284	1.498	1.001	0.887	1.805	1.803	2.036
8	53	M	75		100			+	30.2	35.7	53.3	1.763	1.493	0.726	0.941	1.731	2.384	1.839
9	71	M	75	90				–	16.4	16.5	20.1	1.225	1.223	0.858	0.852	1.425	1.661	1.672
10	64	M	90			CABG		+	26.3	24.5	42.7	1.624	1.742	0.711	0.793	1.564	2.200	1.973
11	67	M		90	90			+	33.6	28.3	37.6	1.117	1.327	1.021	0.894	1.170	1.146	1.309
12	76	F			90		+	+	26.9	18.2	30.7	1.140	1.687	1.402	0.848	1.332	0.950	1.572
13	50	F	99				+	+	25.4	21.8	46.1	1.819	2.119	1.006	0.746	1.967	1.955	2.637
14	52	M			99		+	+	18.4	18.6	33.4	1.817	1.797	0.857	1.166	2.303	2.687	1.976
15	63	M	100	100			+	+	19.1	23.9	35.3	1.849	1.477	1.160	1.602	2.155	1.858	1.345
16	64	F	90	90	90			–	16.6	19.0	28.5	1.719	1.502	1.084	1.224	2.018	1.862	1.648
17	78	M			90			–	21.9	15.7	27.6	1.260	1.753	0.839	0.688	1.882	2.243	2.737
18	65	M			100		+	+	19.0	14.9	27.8	1.464	1.863	1.049	0.992	2.580	2.460	2.601
19	58	F	99	75	75			+	31.9	21.5	46.6	1.460	2.163	1.194	0.856	1.732	1.451	2.024
20	69	M		100	100		+	+	23.0	19.0	32.7	1.420	1.723	0.714	0.665	1.217	1.705	1.829

CAG, Coronary angiography; LAD, left anterior descending artery; LCx, left circumflex artery; RCA, right coronary artery; RV, previous revascularization; MI, previous myocardial infarction; MBFI, myocardial blood flow index; MFR, myocardial flow reserve; CABG, bypass surgery; PTCA, angioplasty; SPET +, myocardial ischemia on SPET images

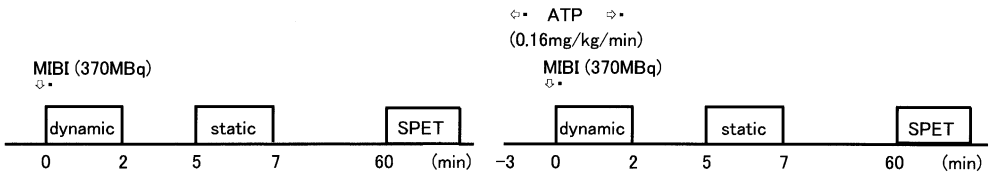

Fig. 1. Study protocol for ^{99m}Tc-sestamibi myocardial scintigraphy

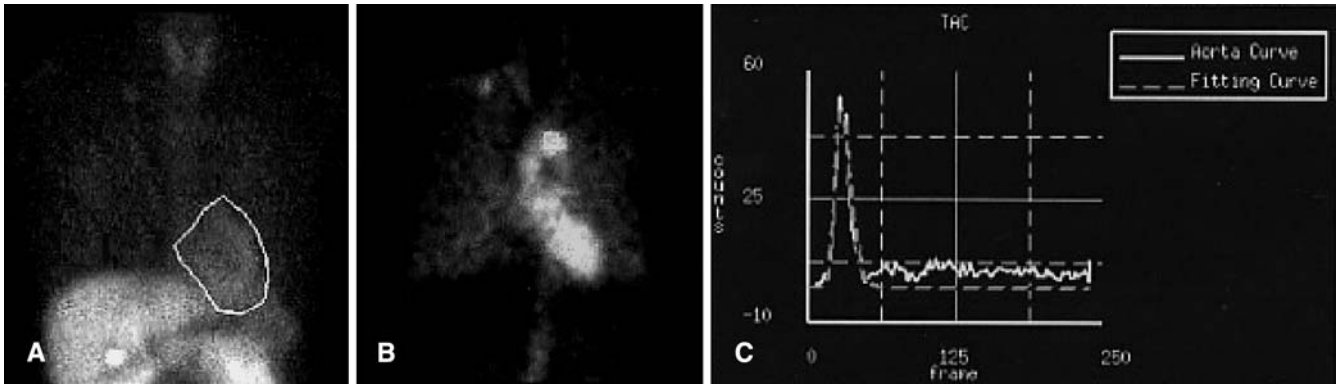

Fig. 2A–C. ROIs and time-activity curve. The ROIs drawn in the myocardial region on the planar static images (**A**) and in the aortic arch on the summed image of the aortic phase of first-pass images (**B**) are shown. The time integral of the first-pass ^{99m}Tc-sestamibi counts was obtained as an area under the gamma-variate-fitted aortic time-activity curve for the aortic region of interest (**C**)

Materials and methods

Patients. This study included 20 patients with angiographically documented CAD (16 males, 4 females; 65.3±9.6 years old) and a control group comprising nine normal volunteers (8 males, 1 female; 38.3±10.9 years old) with a <1% likelihood of CAD based on the age, gender, and clinical symptoms (Table 1). Nine patients had single-vessel CAD, seven patients had two-vessel CAD, and four patients had three-vessel CAD. Eight patients had a previous myocardial infarction. Previous coronary revascularization had been performed in four patients, in two cases by angioplasty and in two by coronary artery bypass grafting (CABG).

PET studies performed within 2 weeks of the sestamibi myocardial perfusion scintigraphy were included in this study and analyzed. No clinical events or changes in medication occurred between the sestamibi and PET studies. All participants were carefully instructed to refrain from caffeine intake during the 24 h before the PET study and the sestamibi study under adenosine triphosphate (ATP) stress. All of them gave written informed consent and this study was approved by the Ethics Committee of Hokkaido University Hospital.

^{99m}Tc-sestamibi imaging protocol and data analysis. ^{99m}Tc-sestamibi angiography and SPET were performed using a 2-day rest-stress imaging protocol (Fig. 1). The planar dynamic images were used to estimate myocardial counts and dynamic counts of blood pool activities, whereas SPET images were used for to estimate left ventricular mass. At rest, just after a bolus injection of 370 MBq ^{99m}Tc-sestamibi into the right medial antecubital vein followed by flushing with 16 ml saline, first-pass radionuclide angiographic data were obtained from the anterior view every 50 ms for 50 s and every 500 ms for 70 s using a large field of view gamma camera equipped with a high-resolution collimator. Stress was induced by infusion of ATP at a rate of 0.16 mg kg^{-1} min^{-1} for 5 min though the left antecubital vein [8, 9]. Three minutes after the start of ATP infusion, planar imaging was performed for 2 min with the patient in the same position for 5 min. Data were acquired using 64×64 matrices with energy discrimination centered at 140 keV with a 20% window. Sixty minutes later, SPET was performed with a dual-head gamma camera SPET system equipped with high-resolution collimators (Vertex; ADAC Laboratories, Milpitas, Calif.). A total of 32 projection images were obtained in a 64×64 matrix over 180°, at 60 s per step. The projection data were prefiltered with a two-dimensional Butterworth filter (order 2.5, critical frequency 0.22 cycles/pixel; and pixel size 0.64 cm) and reconstructed with filtered back-projection (ramp filter) and no attenuation correction. The spatial resolution was about 12 mm full-width at half-maximum (FWHM) after reconstruction.

The myocardial count (C_m, cpm) for 1 min was obtained from the planar static image at 5 min after injection of ^{99m}Tc-sestamibi (Fig. 2). First-pass angiographic data were analyzed to obtain the time integral of the first-pass ^{99m}Tc-sestamibi counts for the aorta. On the summed image (3- to 4-s duration) of the aortic phase of first-pass images, a 2×2 pixel region of interest (ROI) was set on the aortic arch (Fig. 2). The time integral of the first-pass ^{99m}Tc-sestamibi counts was obtained as an area under the gamma-variate-fitted aortic time-activity curve (aorta ACU, counts/cm^2 per minute) for the aortic ROI [10] (Fig. 2). For measurement of the time integral of the aortic counts during ATP stress, the same aortic ROI was applied. The left ventricular myocardium was delineated automatically by the edge where the count was 40–50% of the left ventricular myocardium peak count. The weight of the left ventricular myocardium (M, g) was calculated by the volume of the left ventricular myocardium, having set myocardial gravity to 1.05. The myocardial blood flow index (MBFI) was obtained using the formula:

$$\text{MBFI} = C_m/\text{aorta ACU} \times 100/M \quad (1)$$

Because the baseline MBF is closely related to the rate-pressure product (RPP), MBFI at rest was corrected for the RPP, an index

of myocardial oxygen consumption, by the following equation [11, 12]:

$$\text{Corrected MBFI} = \text{MBFI} \times (\text{mean RPP at rest in PET study}/\text{ind}$$

MFR was calculated as the ratio of MBFI during ATP infusion to MBFI at rest.

Quantitative analysis of MBF using ^{99m}Tc-sestamibi. MBF can be calculated by Sapirstein's principle [13] as follows:

$$\text{MBF} = \text{CO} \times C_m/\text{total ID} \quad (2)$$

where CO = cardiac output and ID = injected dose. The CO was obtained as the ID to the area under the gamma-variate-fitted aortic time-activity curve (aorta ACU) on the basis of the Stewart-Hamilton principle. MBF is calculated from the formula:

$$\text{MBF} = k_1 \times (\text{ID}/\text{aorta ACU}) \times k_2 \times C_m/\text{ID} = k_1 \times k_2 : \quad (3)$$

K_1 and k_2 are the correction factors for the counting rate from the myocardium and the aortic time-activity curve, and the extraction fraction of ^{99m}Tc-sestamibi, respectively, including the attenuation factor, partial volume effect, and sensitivity of the gamma camera. The edge of the left ventricular myocardium was delineated automatically on the short-axis SPET images by the threshold method. The weight of the left ventricular myocardium (M, g) was estimated by the volume of the left ventricular myocardium with a myocardial gravity of 1.05. The myocardial blood flow index (MBFI) was obtained from Eq. 1.

PET protocol and data analysis. MBF at rest and during ATP infusion was calculated by PET using [^{15}O]H_2O. All PET scans were performed with an ECAT EXACT HR+ (Siemens/CTI). A transmission scan was performed to correct the photon attenuation for 6 min with a germanium-68 source. Next, the subject inhaled [^{15}O]CO for 1 min. The total inhaled dose in the [^{15}O]CO examination was 2,000 MBq. After inhalation of the tracer, 3 min was allowed to pass for CO to combine with hemoglobin before a static scan lasting for 5 min was started. The spatial resolution was about 7 mm after reconstruction.

^{15}O radioactivity returned to background levels 10–15 min after the blood volume scan. Then [^{15}O]H_2O was infused into an antecubital vein as a slow (2-min) infusion. The administered dose of [^{15}O]H_2O was 500 MBq/min. A 24-frame dynamic PET scan was performed for 6 min, consisting of 18×10-s and 6×30-s frames. Twelve minutes after the first infusion of [^{15}O]H_2O, intravenous drip infusion of ATP (0.16 mg kg^{-1} min^{-1}) was started until the end of the second PET scan using [^{15}O]H_2O, by which images were recorded in the same sequence. Heart rate (HR), blood pressure (BP) and a 12-lead ECG were recorded at rest and at 1-min intervals during and after the administration of ATP.

All emission sinograms were reconstructed with filtered backprojection using a Hann filter (cut-off frequency 0.3 cycles/pixel). The in-plane resolution was 4.5 mm FWHM in images reconstructed into a 128×128 matrix. All data were corrected for dead time, decay, and measured photon attenuation.

MBF was quantified using the single tissue compartment model developed by Katoh et al. [14, 15]. All PET data were analyzed by three expert doctors who were blind to the patients' clinical data. All acquisition data were resliced along the myocardial axis using the same parameters. The ROI was set automatically when a point in the left ventricle was clicked on in the CO image. The entire myocardial ROI was decided by subtracting the early-phase image obtained with [^{15}O]H_2O. When the edges of the apex and base of the myocardium were clicked, the entire myocardial ROI was set automatically.

Twenty patients with CAD and nine healthy subjects were assessed based on the MBF at rest, under ATP infusion. HR and systolic BP (SBP) were determined for each subject; and RPP was calculated as HR×SBP. Because the baseline MBF is closely related to RPP, MBF at rest was corrected for the RPP [11], an index of myocardial oxygen consumption, according to the following equation [12]: Corrected MBF = MBF×(mean RPP at rest in PET study/individual RPP). MFR was calculated as the ratio of MBF during ATP infusion to MBF at rest.

Statistical analysis. Continuous variables were expressed as mean±SD, and hemodynamic parameters were compared by the paired t test. The MFRs in normal subjects and patients with CAD were compared by the unpaired t test. $P<0.05$ was considered statistically significant.

Results

Hemodynamic response

Hemodynamic data are summarized in Table 2. With ATP stress, significant increases in heart rate and rate-pressure product were found, with a significant decrease in systolic blood pressure in the sestamibi and PET studies. No significant differences between the sestamibi and PET studies were found in heart rate although the systolic blood pressure and rate-pressure product were slightly higher in the sestamibi study than in the PET study.

Relationship between MBFI measured by sestamibi and by PET

The data acquisition and analysis was successful in each subject. Figure 3 shows the correlation between

Table 2. Hemodynamic data

	PET (rest)	PET (ATP)	MIBI (rest)	MIBI (ATP)
SBP (mmHg)	117.9±16.9	107.3±11.2*	123.6±11.7	113.6±12.9*,**
HR (/min)	65.1±11.2	79.1±11.7*	67.2±10.9	79.3±11.2*
RPP	7,680.0±1,729.9	8,496.4±1,548.6*	8,278.9±1,373.5	8,986.9±1,507.2*,**

SBP, Systolic blood pressure; HR, heart rate; RPP, rate-pressure product
*$P<0.01$ vs rest, **$P<0.01$ vs PET

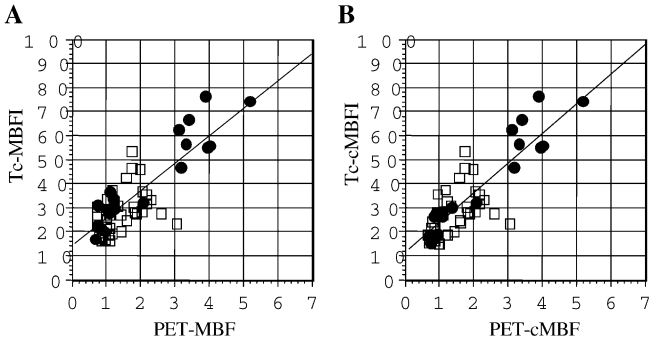

Fig. 3A, B. Relationship between MBFI measured with sestamibi and MBF measured by PET. ●, Normal group; □, CAD group. Good linear correlations were found between MBFI measured with sestamibi and MBF measured by PET (**A**, MBFI= 13.174+11.732×MBF, r=0.821, P<0.001), and between corrected MBFI measured with sestamibi and corrected MBF measured by PET (**B**, cMBFI=10.592+12.546×cMBF, r=0.845, P<0.001)

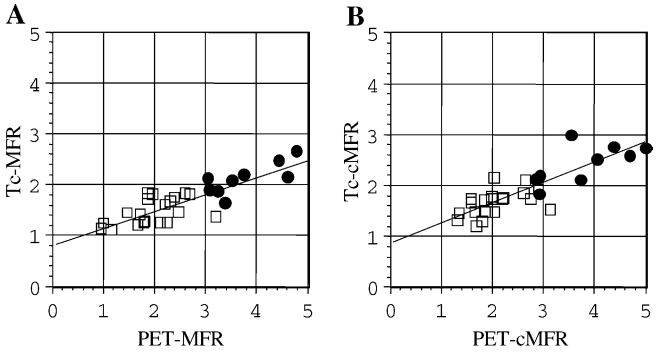

Fig. 4A, B. Relationship between MFR measured with sestamibi and MFR measured by PET. ●, Normal group; □, CAD group. Good linear correlations were found between MFR measured with sestamibi and MFR measured by PET (**A**, Tc-MFR=0.849+ 0.331×PET-MFR, r=0.845, P<0.001), and between corrected MFR measured with sestamibi and corrected MFR measured by PET (**B**, Tc-cMFR=0.916+0.383×PET-cMFR, r=0.843, P<0.001)

the MBFI measured by sestamibi and the MBF measured by PET. The MBFI and MBF showed a good linear correlation (MBFI=13.174+11.732×MBF, r=0.821, P<0.001). When the MBFI and MBF at rest were corrected by the rate-pressure product, the coefficient of correlation between MBFI and MBF increased slightly (corrected MBFI=10.592+12.546×corrected MBF, r=0.845, P<0.001).

Relationship between MFR measured by sestamibi and by PET

In Fig. 4, the MFR measured with sestamibi ($MFR_{sestamibi}$) was plotted against the MFR measured by PET (MFR_{PET}). The MFR measured with sestamibi and MFR measured by PET showed a good linear correlation ($MFR_{sestamibi}$=0.849+0.331×MFR_{PET}, r=0.845, P<0.001). But the MFR with sestamibi was signifi-cantly underestimated. When the MBFI and MBF at rest were corrected by the rate-pressure product, a high correlation coefficient was obtained (cTc-$MFR_{sestamibi}$=0.916+0.383× $cMFR_{PET}$, r=0.843, P<0.001).

Comparison of MFR measured with sestamibi in normal subjects and in patients with CAD

The MFR measured with sestamibi in patients with CAD was significantly lower than that in normal subjects (CAD: 1.484±0.256 vs normal: 2.127±0.308, P<0.001). When the MBFI and MBF at rest were corrected by the rate-pressure product, the MFRs in both patients with CAD and normal subjects were increased, though the MFR in patients with CAD was significantly lower than that in normal subjects (CAD: 1.670±0.251 vs normal: 2.431±0.380, P<0.001).

Detection of CAD using MFR measured by PET and sestamibi

The MFR measured by PET ranged from 0.950 to 3.196 (mean 1.967±0.575) in CAD, and 3.040 to 4.777 (mean 3.758±0.677) in normal subjects. The MFR measured with sestamibi ranged from 1.117 to 1.849 (mean 1.484±0.256) in CAD, and from 1.645 to 2.657 (mean 2.131±0.308) in normal subjects.

When the cut-off point for abnormalities was set at 2.8 for MFR measured by PET, the sensitivity for the detection of CAD was 95% (19/20) and the specificity, 100% (9/9). When the cut-off point was set at 1.8 for MFR measured with sestamibi, the sensitivity was 80% (16/20) and the specificity, 89% (8/9). The stress perfusion SPET images provided similar sensitivity (70%, 14/20) and specificity (89%, 8/9) (Table 1).

Discussion

This study indicates that the MBFI and MFR estimated by dynamic acquisition with ^{99m}Tc-sestamibi correlate well with the values measured by PET. Thus, this new method has the potential for wide application in patients with diffuse CAD. Despite the good linear correlation between the values measured using our method and those measured using PET, the values obtained using sestamibi represented significant underestimates. On the other hand, when the optimal threshold of MFR was used, our method provided high sensitivity and specificity for the detection of CAD. This quantitative assessment may have additional diagnostic value in SPET imaging.

The value of MFR measurement has been well recognized. Gould and Lipscomb [16] originally recognized the

importance of measuring coronary flow reserve (CFR) in clinical practice and were the first to define the relationship between CFR and the severity of stenosis. A $[^{15}O]H_2O$ PET study suggested that MFR decreased and coronary vascular resistance increased in relation to the number of risk factors [17]. In particular, patients with hypercholesteremia and anatomically normal coronary arteries showed a decreased MFR, as measured by nitrogen-13 ammonia PET [18]. MFR was also reduced in patients with diabetes mellitus [19]. These data suggested that reduced MFR may be due to an abnormality in the regulation of coronary flow and preclinical atherosclerosis. Therefore, measurements of MFR are useful in assessing the functional significance of coronary artery stenosis and in predicting diffuse coronary atherosclerosis and microvascular dysfunction. The most widely employed invasive method to measure CFR is use of an intravascular Doppler ultrasound transducer or pressure transducer technique [20], whereas the most frequent noninvasive method for quantification of regional blood flows is PET with $[^{15}O]H_2O$ or ^{13}N-ammonia [14, 21, 22, 23]. However, these techniques have limited value for routine clinical studies because of their high cost and complicated procedures. Therefore, a simple noninvasive assessment of MFR using ^{99m}Tc-labeled tracers would enhance the clinical significance of myocardial SPET imaging.

In patients with multivessel disease, perfusion SPET may not be able to detect stress-induced perfusion abnormalities owing to diffuse reduction of flow. A quantitative estimate of MFR may overcome this limitation of SPET imaging. Recently there have been a number of attempts to estimate MFR using routinely performed SPET tracers [6, 7]. These studies have used dynamic data acquisition with calculation on the basis of the Stewart-Hamilton principle to estimate MBF and MFR. However, they did not validate the estimated values against those obtained by PET measurement.

The current method employed similar methods to estimate MBF and MFR using planar and SPET imaging after ^{99m}Tc-sestamibi administration. This approach is based on the microsphere method, assuming that ^{99m}Tc-sestamibi is taken up by myocardial tissue according to blood flow. MBF is calculated as the ratio of the counts in the tissue to the integral of the arterial concentration of the tracer up to the time of imaging based on the Sapirstein method and the Stewart-Hamilton principle. Serial planar imaging was performed to measure the arterial concentration. A number of physical factors limit accurate estimates of myocardial counts and arterial counts by images, such as attenuation, scatter, and partial volume effects. But most of these factors may be canceled out by calculating the ratio of the counts in the tissue to the integral of the arterial concentration of the tracer.

In this model, arterial input function should be estimated both at rest and during ATP stress. We measured the area under the time-activity curve of the measured first transit counts in the ascending aorta by dynamic planar imaging. The ascending aorta was used since this technique may have the potential for greater reproducibility and be less dependent on the bolus administration than is measurement of the first transit counts in the pulmonary artery, as in Sugihara's method [7]. On the other hand, our method might have the potential to cause a relatively large error in patients who have low cardiac output with a very slow time-activity curve of the aorta. In the present study, however, none of the patients showed an inadequate time-activity curve of the ascending aorta due to poor bolus or impaired left ventricular function. The estimation of cardiac output by radionuclide angiography has been well validated [10].

This model estimated the MBF of the whole heart (the area in the ROI). To estimated the absolute unit of MBF as ml/min per gram tissue, the myocardial mass should be calculated. We estimated the left ventricular myocardial mass by means of SPET images. The threshold method for SPET images was used to calculate left ventricular muscle volume in this study. However, we did not validate the muscle volume measurement with our method by comparing it with measurements using other methods. It therefore cannot be ruled out that our approach caused a significant error in MBFI. However, this factor will have been canceled out in the MFR calculation, because left ventricular muscle weights at rest and during ATP stress were the same.

One of the major limitations in this study was underestimation of the MFR value. In canine experimental models, the initial distribution of sestamibi under basal conditions correlated closely with regional blood flow, but when sestamibi was administered at a flow rate >2–3 ml min^{-1} g^{-1}, its uptake or retention plateaued [23, 24, 25]. In humans, Taki et al. [6] reported that the increase in myocardial sestamibi uptake underestimated the increase in blood flow, especially at higher flow rates, since sestamibi retention reached a plateau at threefold the baseline blood flow. This was due to a significant reduction in the extraction fraction in the high flow range with SPET perfusion tracers compared with $[^{15}O]H_2O$. However, the diagnosis of CAD may be permitted by use of a certain threshold of MFR measured by ^{99m}Tc-sestamibi, given that the MFR in patients with CAD was significantly lower than that in normal subjects in our study.

In this investigation, the systolic blood pressure and rate-pressure product in the ^{99m}Tc-sestamibi study were slightly higher than those in the PET study. These differences may have derived from the difference in time from the beginning of study (in PET, CO gas study is performed before measurement of MBF using water). We calculated MBFI values after correction for rate-pressure product because the baseline MBF is closely related to rate-pressure product. Slightly higher correlation coefficients were obtained between MBF by PET and MBFI using sestamibi when MBF and MBFI at rest were corrected by rate-pressure product.

In this study included MBFI and MFR were measured in the whole left ventricle. On the other hand, regional MFR analysis is required for detection of regional myocardial ischemia in CAD patients. Such analysis is possible via estimation of the fractional distribution on SPET images. Further investigation may be required in this respect.

Conclusion

We have developed a noninvasive method to quantitatively estimate MBF and MFR using ^{99m}Tc-sestamibi by taking into account the arterial input function. The MBFI and MFR measured with sestamibi showed a good linear correlation with those obtained by PET, but MFR using sestamibi was underestimated. Quantitative assessment may have additional diagnostic value in SPET imaging to predict diffuse coronary atherosclerosis and preclinical microvascular dysfunction.

Acknowledgements. We would like to thank Kenichi Nishijima, MS, for excellent work in providing PET tracers. We are also grateful to Kotaro Suzuki, RT, for handling SPET and PET imaging.

References

1. Heller GV, Herman SD, Travin MI, Baron JI, Santos-Ocampo C, McClellan JR. Independent prognostic value of intravenous dipyridamole with technetium-99m sestamibi tomographic imaging in predicting cardiac events and cardiac-related hospital admissions. *J Am Coll Cardiol* 1995; 26:1202–1208.
2. Stratmann HG, Tamesis BR, Younis LT, Wittry MD, Amato M, Miller DD. Prognostic value of predischarge dipyridamole technetium-99m sestamibi myocardial tomography in medically treated patients with unstable angina. *Am Heart J* 1995; 130:734–740.
3. Nicolai E, Cuocolo A, Pace L, et al. Adenosine coronary vasodilation quantitative technetium 99m methoxy isobutyl isonitrile myocardial tomography in the identification and localization of coronary artery disease. *J Nucl Cardiol* 1996; 3:9–17.
4. Miller DD, Younis LT, Chaitman BR, et al. Diagnostic accuracy of dipyridamole technetium 99m-labeled sestamibi myocardial tomography for detection of coronary artery disease. *J Nucl Cardiol* 1997; 4:18–24.
5. Sharir T, Germano G, Kavanagh PB, Lai S, Cohen I, Lewin HC, Friedman JD, Zellneger MJ, Berman DS. Incremental prognostic value of post-stress left ventricular ejection fraction and volume by gated myocardial perfusion single photon emission computed topography. *Circulation* 1999; 100: 1035–1042.
6. Taki J, Fujino S, Nakajima K, Matsunari I, Okazaki H, Saga T, Bunko H, Tonami N. ^{99m}Tc-sestamibi retention characteristics during pharmacologic hyperemia in human myocardium; comparison with coronary flow reserve measured by Doppler flow wire. *J Nucl Med* 2001; 42:1457–1463.
7. Sugihara H, Yonekura Y, Kataoka K, Fukai D, Kitamura N, Taniguchi Y. Estimation of coronary flow reserve with the use of dynamic planar and SPECT images of Tc-99m tetrofosmin. *J Nucl Cardiol* 2001; 8:575–579.
8. Miyagawa M, Kumano S, Sekiya M, et al. Thallium-201 myocardial tomography with intravenous infusion of adenosine triphosphate in diagnosis of coronary artery disease. *J Am Coll Cardiol* 1995; 26:1196–1201.
9. Watanabe K, Sekiya M, Ikeda S, Miyagawa M, Kinoshita M, Kumano S. Comparison of adenosine triphosphate and dipyridamole in diagnosis by thallium-201 myocardial scintigraphy. *J Nucl Med* 1997; 38:577–581.
10. Sugihara H, Yonekura Y, Miyazaki Y, Taniguchi Y. Estimation of cardiac output by first-pass transit of radiotracers. *Ann Nucl Med* 1999; 13:299–302.
11. Czenin J, Muller P, Chan S, et al. Influence of age and hemodynamics on myocardial blood flow and flow reserve. *Circulation* 1993; 88:62–69.
12. Marinho NVS, Keogh BE, Costa DC, Lammerstma AA, Ell PJ, Camici PG. Pathophysiology of chronic left ventricular dysfunction; new insights from the measurement of absolute myocardial blood flow and glucose utilization. *Circulation* 1996; 93:737–744.
13. Sapirstein LA. Regional blood flow by fractional distribution of indicators. *Am J Physiol* 1958; 193:161.
14. Katoh C, Ruotsalainen U, Laine H, et al. Iterative reconstruction based on median root prior in quantification of myocardial blood flow and oxygen metabolism. *J Nucl Med* 1999; 40:862–867.
15. Iwado Y, Yoshinaga K, Furuyama H, et al. Decreased endothelium-dependent coronary vasomotion in healthy young smokers. *Eur J Nucl Med* 2002; 29:984–990.
16. Gould KL, Lipscomb K. Effects of coronary stenoses on coronary flow reserve and resistance. *Am J Cardiol* 1974; 34:48–55.
17. Pitkanen OP, Raitakari OT, Ronnemaa T, et al. Influence of cardiovascular risk status on coronary flow reserve in healthy young men. *Am J Cardiol* 1997; 79:1690–1692.
18. Yokoyama I, Ohtake T, Momomura S, Nishikawa J, Sasaki Y, Omata M. Reduced coronary flow reserve in hypercholesterolemic patients without overt coronary stenosis. *Circulation* 1996; 94:3232–3238.
19. Yokoyama I, Momomura S, Ohtake T, Yonekura K, Nishikawa J, Sasaki Y, Omata M. Reduced coronary flow reserve in non-insulin-dependent diabetes mellitus. *J Am Coll Cardiol* 1997; 30:1472–1477.
20. Doucette JW, Cori PD, Payne HM, et al. Validation of a Doppler guide wire for intravascular measurement of coronary artery flow velocity. *Circulation* 1992; 85:1899–1911.
21. Hutchins GD, Schwaiger M, Rosenspire KC, Krivokapich J, Schelbert H, Kuhl DE. Noninvasive quantification of regional blood flow in the human heart using N-13 ammonia and dynamic positron emission tomographic imaging. *J Am Coll Cardiol* 1990; 15:1032–1042.
22. Kaufmann PA, Gnecchi-Ruscone T, Yap JT, et al. Assessment of the reproducibility of baseline and hyperemic myocardial blood flow measurements with oxygen-15 labeled water and PET. *J Nucl Med* 1999; 40:1848–1856.
23. Okada RD, Glover D, Gaffney T, Williams S. Myocardial kinetics of techetium-99m-hexakis-2-methoxy-2-methylropylisonitrile. *Circulation* 1988; 77:491–498.
24. Glover DK, Okada RD. Myocardial kinetics of Tc-MIBI in canine myocardium after dipyridamole. *Circulation* 1990; 81: 628–637.
25. Melon PG, Beanlands RS, DeGrado TR, Nguyen N, Petry NA, Schwaiger M. Comparison of technetium-99m sestamibi and thallium-201 retention characteristics in canine myocardium. *J Am Coll Cardiol* 1992; 20:1277–1283.